various aspects of the boundary layers developing behind the shock wave propagating along the perforated walls, because the important information we should have for the next research program comes mainly from the first parts of the boundary layer.

References

[1] Szumowski, A. P., "Attenuation of a Shock Wave along a Perforated Tube," *Shock Tube Research*, Chapman and Hall, London, 1971, pp. 14/1–14/10.

[2] Wu, J. H. T. and Ostrowski, P. P., "Shock Attenuation in a Perforated Duct," *Shock Tube Research*, Chapman and Hall, London, 1971, pp. 15/1–15/14.

[3] Honda, M., Takayama, K., and Onodera, O., "Studies on the Motion of Shock Waves Propagating along Perforated Ducts," *Report Institute High Speed Mechanics, Tohoku Univ.*, Vol. 30, No. 272, 1974.

[4] Mirels, H., "Boundary Layer Behind Shock or Thin Expansion Wave Moving into Stationary Fluid," TN 3712, 1956, NACA.

[5] Dorrance, W. H., *Viscous Hypersonic Flow*, McGraw-Hill, New York, 1962, pp. 26–32.

Axial Flow Measurements in Trailing Vortices

D. L. CIFFONE* AND K. L. ORLOFF†

NASA Ames Research Center, Moffett Field, Calif.

A SCANNING laser Doppler velocimeter[1–3] was used to measure the axial velocity defect in the cores of trailing vortices behind a lifting airfoil of rectangular planform. Data were obtained at several different angles of attack and downstream distances ranging from 30 to 10^3 chord lengths. The experiment was performed at the Univ. of California's water tow-tank facility at Richmond, Calif. The tank is 61 m long, 2.44 m wide, and 1.7 m deep. The test Reynolds number based on the wing chord was nominally 2.43×10^5. The wing used has an NACA 0015 airfoil section, an aspect ratio of 5.33, and a span of 0.61 m.

The existence of axial flow in the cores of lift-generated trailing vortices has been established experimentally,[2–8] with both defects and enhancements of the axial velocity being reported. With the exception of the water tank hydrogen bubble measurements of Ref. 7 and limited flight-test data, the experiments have been restricted to near field vortex characteristics. The present test was designed to obtain continuous data from the near field into the far field while removing uncertainties associated with the interpretation of data obtained by the hydrogen bubble technique. A detailed description of the present test procedure and data analysis is given in Ref. 8.

Batchelor[9] deduced the way in which the gradual slowing down of the rotary motion of the vortex by viscous action leads to an increased pressure at the core axis, resulting in an axial deceleration of the core fluid. He presents these effects explicitly in a similarity solution that is valid very far downstream. Brown,[10] using a modified Betz[11] calculation to describe the vortex flowfield, shows that the incremental axial velocity can be either forward or rearward, depending on the lift and profile drag coefficients of the wing. However, in contrast to Batchelor's work, Brown's results are expected to be valid only at relatively short distances behind the airfoil where the spiraling vortex is well rolled-up, but before the vorticity has been greatly spread and reduced in intensity by turbulent diffusion.

Moore and Saffman[12] consider the structure of a laminar trailing vortex behind a lifting wing and introduce viscosity to remove core centerline singularities, allowing the structure of the viscous core to be obtained. The pressure in the viscous core is then determined and used to calculate the axial velocities produced by streamwise pressure gradients. It is shown that the axial velocity can have a perturbation either away from or toward the wing, depending on the distribution of tip loading on the wing. The axial flow deficit in the core due to the presence of a boundary layer on the wing is also taken into account. For an isolated vortex from the tip of a rectangular planform wing with elliptic tip loading, the following approximate relationship (slightly modified from Ref. 12) is derived for the axial velocity at the core centerline V_x, normalized by the freestream velocity U_∞

$$\frac{V_x}{U_\infty} = (1 + 8.57 \times 10^{-5} \alpha^2 Re_c^{1/2}) \frac{0.28}{(x/c)^{1/2}} \tag{1}$$

where α is the angle of attack (in deg), Re_c is the Reynolds number based on a wing chord, and x/c is the downstream distance (in chord lengths). The derivation of Eq. (1) utilizes the approximation that $V_x \ll U_\infty$.

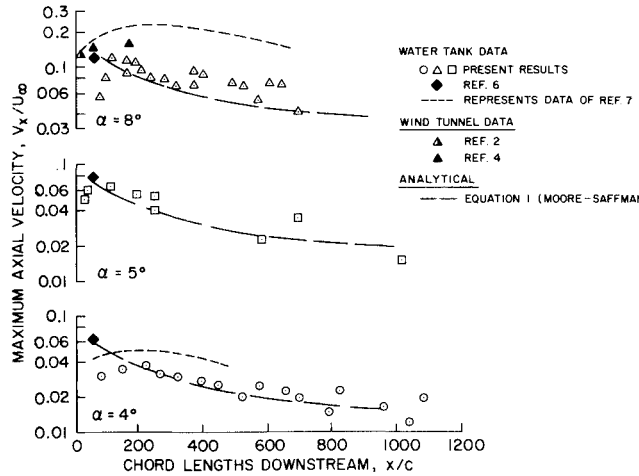

Fig. 1 Variation of maximum axial velocity with downstream distance; comparison of measurements with the laminar prediction of Moore and Saffman.[12]

Figure 1 compares the measured values of V_x/U_∞ with those predicted by Eq. (1). The agreement is remarkably good over the entire range of downstream distances, which supports the credibility of calculating axial velocities using the results of Moore and Saffman. Shown for comparison are the water tank data of Refs. 6 and 7 and the wind-tunnel data of Refs. 2 and 4. Agreement between the laminar prediction and the data improves as the angle of attack (α) decreases. This result is believed to be a consequence of the approximation that $V_x \ll U_\infty$ in the analysis.

References

[1] Grant, G. R. and Orloff, K. L., "A Two-Color, Dual Beam Backscatter Laser Doppler Velocimeter," TM X-62,254, 1973, NASA.

[2] Orloff, K. L. and Grant, G. R., "The Application of Laser Doppler Velocimetry to Trailing Vortex Definition and Alleviation," TM X-62,243, 1973, NASA.

[3] Ciffone, D. L., Orloff, K. L., and Grant, G. R., "Laser Doppler Velocimeter Investigation of Trailing Vortices Behind a Semi-Span Swept Wing in a Landing Configuration," TM X-62,294, 1973, NASA.

[4] Chigier, N. A. and Corsiglia, V. R., "Wind-Tunnel Studies of Wing Wake Turbulence," *Journal of Aircraft*, Vol. 9, No. 12, Dec. 1972, pp. 820–825.

[5] Logan, A. H., "Vortex Velocity Distributions at Large Downstream Distances," *Journal of Aircraft*, Vol. 8, No. 11, Nov. 1971, pp. 930–932.

[6] Olsen, J. H., "Results of Trailing Vortex Studies In a Towing Tank," in *Aircraft Wake Turbulence and Its Detection*, edited by J. H. Olsen, A. Goldberg, and M. Rogers, Plenum, New York, 1971, p. 455.

[7] Lezius, D. K., "Study of the Far Wake Vortex Field Generated by a Rectangular Airfoil in a Water Tank," TM X-62,274, 1973, NASA.

[8] Orloff, K. L., Ciffone, D. L., and Lorincz, D., "Airfoil Wake Vortex Characteristics in the Far Field," TM X-62,318, 1973, NASA.

[9] Batchelor, G. K., "Axial Flow in Trailing Line Vortices," *Journal of Fluid Mechanics*, Vol. 20, 1964, pp. 645–658.

Received January 21, 1974.

Index category: Jets, Wakes, and Viscid-Inviscid Flow Interactions.

* Research Scientist.

† Research Scientist. Associate Member AIAA.

[10] Brown, C. E., "Aerodynamics of Wake Vortices," *AIAA Journal*, Vol. 11, No. 4, April 1973, pp. 531–536.
[11] Betz, A., "Behavior of Vortex Systems," TM 713, 1933, NACA.
[12] Moore, D. W. and Saffman, P. G., "Axial Flow in Laminar Trailing Vortices," *Proceedings of the Royal Society* (London), Ser. A, Vol. 333, 1973, pp. 491–508.

Finite-Thickness Diffusion Flames over a Pyrolyzing Fuel Plate

HAROLD KERZNER* AND HERMAN KRIER†
University of Illinois at Urbana-Champaign, Urbana, Ill.

Nomenclature

B = nondimensional heat feedback ratio[3]
C_p = specific heat of a gas species, cal/g°K
f = nondimensional stream function
f' = nondimensional velocity = u/u_e
K_1 = nondimensional surface blowing parameter[3]
K_2 = nondimensional surface activation energy ($K_2 = E_w RT_e$)
l = density-viscosity ratio = $\rho\mu/\rho_e\mu_e$
$\hat{M}$ = molecular weight, g/g-mole
m, n = order of reaction for oxidizer and fuel, respectively
Q = flame heat release, cal/g
T = temperature, °K
u = x-component of velocity, cm/sec
v = y-component of velocity, cm/sec
Y = mass fraction
α_{ox} = oxygen/fuel ratio at flame sheet
α_T = nondimensional heat release, $Q/C_p T_e$
β = pressure gradient parameter[3]
ζ_g = Damköhler number[2]
η = transformed y-component
θ = nondimensional temperature, T/T_e
μ = absolute coefficient of viscosity
ν', ν'' = stoichiometric coefficients
ρ = density, g/cm³
ϕ = fuel/oxygen mass ratio (stoichiometric ratio)

Subscripts

e = boundary-layer edge
$( )_\eta$ = differentiation with respect to η
$( )_s$ = differentiation with respect to s
w = wall (fuel surface)
i = species index
F = fuel
ox = oxidizer
∞ = freestream conditions
$+$ = upper side of fuel wall
$-$ = lower side of fuel wall

Introduction

THE analysis of chemically reacting viscous flows has been greatly simplified by considering the limiting cases of equilibrium and frozen flow. The reader is referred to the classical monographs by Lees[1] and Chung.[2] For equilibrium flow, as the Damköhler number,‡ ζ_g, approaches infinity, the infinitely thin flame sheet is generated defining the streamline where the fuel and oxidizer concentrations are zero and where a heat and mass source exist. For frozen flows, as the Damköhler number approaches zero, a nonreacting flow limit is defined. Thus, for frozen and equilibrium flows, an explicit source term in the energy and species equations is eliminated. For a detailed analysis of the physical phenomena, see Krier and Kerzner.[3]

In the present case, the fuel is assumed to undergo surface pyrolysis with the chemical reactions represented by Arrhenius Kinetics of second order. The effects of the finite thickness of the flame are characterized by a variable gas-phase Damköhler number. These effects are in addition to the "blowing" effect of the gas added to the boundary layer. Although it can be shown that reactive boundary layers with mass addition do not generally admit similar solutions, such an approximate analysis is presented with results that interpret the physico-chemical processes in the boundary layer.

There are generally two studies of interest in the analysis of finite chemical thermodynamics coupled to flow phenomena. First, the relative thickness of the diffusion flame is a complex function of the Damköhler number. Secondly, one attempts to determine the exact limiting numerical values of Damköhler numbers which reflect either frozen or equilibrium flow.

Governing Equations

The conservation equations that are employed to simulate finite kinetics may be written as

$$(lf_{\eta\eta})_\eta + \beta[(\rho_e/\rho) - f_\eta^2] = 0 \tag{1}$$

$$(lY_{i\eta})_\eta + fY_{i\eta} - \zeta_g \frac{\hat{M}_i}{\hat{M}} (\nu_i' - \nu_i'') e^{-E/RT} \frac{\rho}{\rho_e}^{m+n-1} Y_f^{\,n} Y_{ox}^{\,m} = 0 \tag{2}$$

$$(l\theta_\eta)_\eta + f\theta_\eta + (\zeta_g Q/C_p T_e)(\rho/\rho_e)^{m+n-1} e^{-E/RT} Y_f^{\,n} Y_{ox}^{\,m} = 0 \tag{3}$$

where

$$\rho_e/\rho = T/T_e = \theta \tag{4}$$

is also employed.

Because of the nonapplicability of the flame sheet, the governing equations are now solved as two-point boundary value problems.§

At $\eta = 0$

$$f(\eta) = K_1 \exp[K_2/\theta(\eta)] \quad (K_1, K_2 \text{ are constants});$$
$$f'(\eta) = 0; \qquad f(\eta) = -B\theta'(\eta);$$
$$Y_f'(\eta) + f(\eta)[Y_f(\eta) - Y_{f-}(\eta)] = 0; \quad Y_{ox}(\eta) = 0 \tag{5}$$

At $\eta \to \infty$

$$f'(\eta) = 1; \qquad Y_{ox}(\eta) = Y_{ox_e}; \qquad \theta(\eta) = 1; \qquad Y_f(\eta) = 0 \tag{6}$$

The numerical scheme for the solution to the governing equations is well known and follows the same procedure as discussed by Krier and Kerzner.[3]

In order to solve the energy and species equations by using a superpositioning procedure, the sources terms must be "quasi-linearized" by assuming that they are known functions of the initial conditions in each iteration. Once solutions for the energy and species equations are found, new iterative solutions are based upon old solutions to the conservation equations.

Results

Figure 1 shows the wall blowing rate vs freestream oxidizer mass fraction for variable Damköhler number. For the case when $\zeta_g = 1$, the flow is frozen, and the wall blowing rate is constant for all values of Y_{ox_e}. As the Damköhler number increases, the wall blowing rate approaches the value of the flame sheet model. Results by Liu and Libby[4] show that for $Y_{ox_e} = 0.23$ and $f_w = -0.045$, frozen flow may be represented by a Damköhler number of 2–5, and equilibrium flow by a Damköhler number of approximately 1000. The results by Liu and Libby, however, were not based upon coupled wall boundary conditions, and numerical breakdown is said to occur for $\zeta_g > 1000$.

In the present study it was found that the wall boundary condition, specifically $f_w = -\beta\theta_{\eta w}$, is the controllng factor in

Received January 25, 1974; revision received March 15, 1974.
Index categories: Boundary Layers and Convective Heat Transfer—Laminar; Reactive Flows.

* Research Assistant, Department of Aeronautical and Astronautical Engineering; presently Associate Scientist, Thiokol Chemical Company, Brigham City, Utah. Member AIAA.
† Associate Professor, Department of Aeronautical and Astronautical Engineering. Member AIAA.

‡ The Damköhler number is the ratio of the characteristic diffusion time to the characteristic chemical reaction time.[2]

§ See Ref. 3, for discussion of the boundary layers used in Eqs. (5) and (6).